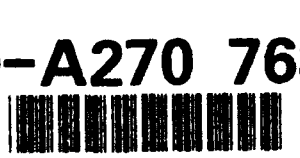

HEAT TRANSFER PERFORMANCE OF A ROOF-SPRAY COOLING SYSTEM EMPLOYING THE TRANSFER FUNCTION METHOD

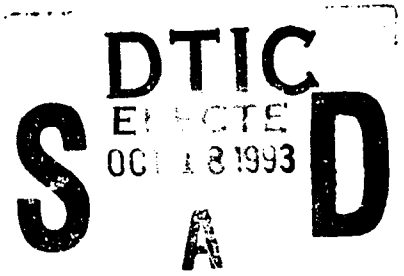

By

JOSEPH A. CLEMENTS

A THESIS PRESENTED TO THE GRADUATE SCHOOL
OF THE UNIVERSITY OF FLORIDA IN PARTIAL FULFILLMENT
OF THE REQUIREMENTS FOR THE DEGREE OF
MASTER OF SCIENCE

UNIVERSITY OF FLORIDA

1993

This thesis is dedicated to my wife, Maria, whose patience and endurance made this thesis possible.

ACKNOWLEDGMENTS

I wish to express my sincere thanks to Dr. S. A. Sherif, Dr. H. A. Ingley III, and Dr. B. L. Capehart for consenting to serve as members of my supervisory committee. The guidance, patience, and encouragement of Dr. Sherif, my committee chairman, have been greatly appreciated.

My graduate education has been funded by the United States Navy's Fully Funded Graduate Education Program. I am most grateful to Captain J. P. Phelan for his generous and skilled assistance in dealing with the Navy that was the key to my being able to maintain my educational funding and remain in Gainesville full-time to complete my degree.

TABLE OF CONTENTS

LIST OF TABLES

LIST OF FIGURES

KEY TO SYMBOLS

A	Area of roof, m^2
A_n	Constants in water saturation pressure/temperature correlation equation
b_n	Conduction transfer function coefficients, $W/(m^2\ ^oC)$
c_n	Conduction transfer function coefficients, $W/(m^2\ ^oC)$
d_n	Conduction transfer function coefficients
h_{evap}	Evaporative heat transfer coefficient, 5.678 $W/(m^2\ K)$
h_i	Internal convective heat transfer coefficient, $W/(m^2\ K)$
h_o	External convective heat transfer coefficient, $W/(m^2\ K)$
n	Summation index
P	Total barometric pressure of moist air, Pa
P_{wa}	Partial pressure of water vapor in moist air, Pa
P_{wr}	Saturation pressure of water at the roof surface, Pa
P_{ws}	Saturation pressure of water vapor, psia or Pa
$q_{cond(roof)}$	Conductive heat flux through roof, W/m^2
$q_{conv(inside)}$	Convective heat flux at inside surface of the roof, W/m^2
$q_{conv(outside)}$	Convective heat flux at outside surface of the roof, W/m^2
$q_{e,\theta}$	Heat gain through roof at calculation hour θ, W/m^2
q_{evap}	Evaporative heat flux, W/m^2

$q_{rad(inside)}$	Radiative heat flux at inside surface of the roof, W/m^2
$q_{rad(outside)}$	Radiative heat flux at outside surface of the roof, W/m^2
q_{solar}	Solar heat flux at outside surface of the roof, W/m^2
R_r	Thermal resistance of roof (m^2 K/W)
T	Temperature, ^{0}R or K
T_a	Ambient outside temperature, ^{0}C or K
T_e	Sol-air temperature, ^{0}C or K
$T_{r,i}$	Temperature of inside surface of the roof, ^{0}C or K
$T_{r,o}$	Temperature of outside surface of the roof, ^{0}C or K
T_{set}	Temperature of inside conditioned space, K
v	Wind speed, k/hr
W	Uncertainty
W_{x_i}	Uncertainty of any variable x_i
α	Absorptance of the surface of the roof for solar radiation
δ	Time interval, h
δR	Difference between the long-wave radiation incident on the surface from the sky and surroundings and the radiation emitted by a blackbody at ambient outdoor air temperature, W/m^2
ε	Emissivity
σ	Stefan-Boltzman constant, 5.6697×10^{-8} W/(m^2 K^4)
θ	Time, h
ω	Humidity ratio of the moist air, $kg_{water}/kg_{dry\ air}$

Abstract of Thesis Presented to the Graduate School
of the University of Florida in Partial Fulfillment of the
Requirements for the Degree of Master of Science

HEAT TRANSFER PERFORMANCE OF A ROOF-SPRAY COOLING SYSTEM EMPLOYING THE TRANSFER FUNCTION METHOD

By

Joseph A. Clements

December, 1993

Chairperson: Dr. S. A. Sherif
Major Department: Mechanical Engineering

Roof-spray cooling systems have been developed and implemented to reduce the heat gain through roofs so that conventional cooling systems can be reduced in size or eliminated. Currently, roof-spray systems are achieving greater effectiveness due to the availability of direct digital controls. The objective of this thesis was to develop a mathematical model of the heat transfer through a roof-spray cooled roof that predicted heat transfer based on existing weather data and roof heat transfer characteristics as described by the Transfer Function Method. The predicted results of this model were compared to the results of existing experimental data from previously conducted roof-spray cooling experiments.

The mathematical model is based on energy balances at the exterior and interior surfaces of the roof construction that include evaporative, convective, radiative, and conductive heat transfer mechanisms. The Transfer Function Method is used to relate the energy balances at the two surfaces that differ in amplitude and phase due to the thermal resistance and thermal capacitance characteristics of the roof.

The combined model yielded moderately good predictions of heat transfer through the roof experimental results for the roof-spray cooled condition. The calculation method shows promise as a relatively simple means of predicting heat gains based on calculation procedures that are similar to those frequently used by many engineers.

CHAPTER 1
INTRODUCTION

Roof-spray cooling systems continue to increase in popularity for a number of reasons. Evaporative roof-spray cooling which has been widely implemented since the 1930s to provide cost effective cooling for industrial applications is now seen as a method to provide cooling which does not add to the depletion of fossil fuels or contribute to possible global warming problems caused by combustion and the use of CFC based refrigerants in traditional vapor compression refrigeration systems. A major advance that has improved the effectiveness of roof-spray cooling is the availability of direct digital controls, which allow water to be applied to roofs to achieve maximum cooling without the application of excessive water.

Many researchers have studied various forms of rooftop evaporative cooling including solar ponds, trickling water, and roof-sprays. In 1940 Houghton et al. [1] studied the effects of roof ponds and roof-sprays on temperature and heat transfer in various roof constructions. In the 1960s, Yellott [2] reported on the effectiveness of a roof-spray cooling system that consisted of little more than a rooftop grid of sprinkler heads and supply pipes with a water supply controlled by a solenoid valve and timer. More recently,

research has been conducted to numerically model roof-spray cooling systems. This includes the work of Tiwari et al. [3], Carrasco et al. [4], Somasundaram and Carrasco [5], and Kondepudi [6].

The heat transfer through roofs with various construction configurations has also been studied extensively. Spitler and McQuiston [7] discussed the latest modeling techniques for the prediction of cooling loads and times as they occur in the zones of a building as a result of the daily loads of ambient temperature and incident solar radiation.

However, a model that incorporates the current modeling of roof systems and roof-spray cooling is lacking. This thesis presents a numerical model for the combined heat transfer response to roof-spray cooling and roof construction in response to the variation of ambient temperature, humidity and solar flux over a typical day and incorporates the effects of thermal capacitance of a roof as modeled by the Transfer Function Method (TFM). The TFM uses conduction transfer functions to predict the heat flux at the inside of the roof as a function of previous values of outside and inside temperatures and heat fluxes. The magnitude and direction of the inside heat flux may be smaller or larger than the heat flux at the outside surface depending on whether the thermal mass of the roof is increasing or decreasing in stored energy. This thesis will present a numerical solution to the heat transfer problem and compare the results to existing experimental data from previously

conducted roof-spray cooling experiments. The heat transfer mechanisms acting on the outside surface in response to ambient temperature and incident solar radiation are evaporation, convection, radiation, and conduction. The transfer mechanisms acting on the inside surface are convection, radiation, and conduction in response to the energy transfer at the outside surface and a fixed room ambient temperature. The energy balances at the two surfaces are related, but the amplitude and phase of the inside energy transfer will depend on the thermal resistance and thermal capacitance characteristics of the roof.

The solution presented should enhance the understanding of the combined effects of evaporative cooling and thermal capacitance of building envelope construction. As a design tool the benefit of this modeling will be that building designers would more easily choose the best combination of roofing, spray-cooling, and conventional cooling systems. This modeling also has an added benefit in that it can be used as a basis for algorithms that determine the most effective and efficient application of roof-spray cooling to a roof.

CHAPTER 2
MATHEMATICAL MODEL

Introduction

The various elements of the heat transfer mechanisms are presented in this chapter. First, the mathematical basis (derived in terms of the energy balances) is presented in the form of equations. The different heat transfer mechanisms and assumptions concerning these mechanisms are also discussed. Second, the thermal capacitance characteristics and effects of the roof system are presented. The different types of roof construction, the heat transfer properties of the materials, and the assumptions concerning these properties are also discussed. Finally the interaction of the heat transfer mechanisms and the construction are discussed and a mathematical basis in the form of equations is presented.

Heat Transfer Mechanisms

Kondepudi [6] and Carrasco et al. [4] presented a thorough development of a mathematical model of the heat transfer mechanisms of a spray cooled roof with some assumptions being made. These assumptions include:

(1) The problem is quasi-steady in response to varying ambient temperatures and solar flux.

(2) An infinitesimally thick film of water is maintained on the roof surface.

(3) The saturated water vapor pressures respond in a linear fashion to temperature.

(4) Wind effects are included in the convective heat transfer model.

(5) Thermal capacitance effects of the roof and water film are neglected.

All of these assumptions with the important exception of the thermal capacitance effects of the roof will be carried through this paper. The initial formulation of the energy balances will ignore the thermal capacitance effects of the roof.

The energy balances for the two interfaces of the process are presented in Figure 2.1. The energy balances at each interface are described below and provide a problem that must be solved simultaneously.

Roof Exterior-Air Interface

As indicated in Figure 2.1 the incident solar energy is dissipated by a combination of evaporative, radiative, convective, and conductive heat transfer.

$$q_{solar}=q_{evap}+q_{rad(outside)}+q_{conv(outside)}+q_{cond(roof)} \qquad (2.1)$$

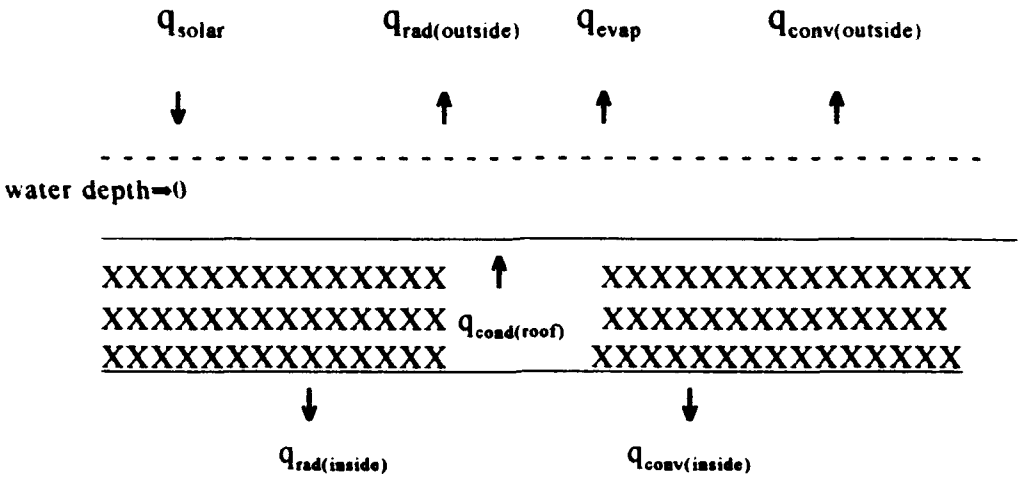

Figure 2.1: Energy balances at roof surfaces

The evaporative heat transfer is a result of Fick's Law of diffusion of the water vapor at the wetted surface diffusing into the ambient air, as presented by Tiwari et al. [3].

$$q_{evap} = 0.013 h_{evap}(P_{wr}-P_{ws}) \qquad (2.2)$$

The partial pressure of water at the roof surface, P_{wr}, is predicted from Mathur's correlation [8] for the water saturation pressure, P_{ws}, as a function of temperature.

$$P_{ws} = A_0 + A_1 T + A_2 T^2 + A_3 T^3 + A_4 T^4$$

where A_0 = 670.2012 psia

A_1 = -5.325521 psia/°R

A_2 = 1.59464 $\times 10^{-2}$ psia/°R^2

A_3 = -0.2134061 $\times 10^{-4}$ psia/°R^3

A_4 = 0.1077853 $\times 10^{-7}$ psia/°R^4

P_{ws} = saturation pressure of water vapor, psia

T = absolute temperature, °R

The partial pressure of water in the ambient air is predicted by ASHRAE [9] as:

$$P_{ws} = (P\omega)/(0.62198 + \omega)$$

where P = total barometric pressure of moist air, Pa

ω = humidity ratio of the moist air, kg_{water}/kg_{air}

$$q_{rad(outside)} = \varepsilon\sigma(T_{r,o}^4 - T_a^4) \qquad (2.3)$$

The equation for the outside radiative heat flux can be refined based on Alford et al. [10], who proposed that the ambient temperature for the radiative heat transfer should be decreased by 2.8 K. This decrease is based on the assumption that all radiation reaching the earth originates in the first 1500 meters of elevation and accounts for a normal atmospheric temperature gradient of about 7 K per 1000 meters elevation. Thus,

$$q_{rad(outside)} = \varepsilon\sigma(T_{r,o}^4 - (T_a - 2.8)^4) \qquad (2.4)$$

Another method of correcting for the difference in net longwave radiation exchange between the roof and the sky is presented by Bliss [11].

Under clear sky conditions the sky-to-surface radiation difference for a horizontal black surface, δR, is typically in the range of 63 to 95 W/m^2. This radiation difference is a function of elevation, cloudiness, air temperature near the ground, and the dew point, but will be assumed to be an average of 63 W/m^2 for clear sky conditions at the experiment sites of Bryan, Texas and Pittsburgh, Pennsylvania. Bliss' model will be used in the predicted heat flux calculations in this report.

The convective and conductive heat fluxes at the outside roof surface are given by the following two equations:

$$q_{conv(outside)}=h_o(T_{r,o}-T_a) \tag{2.5}$$

$$q_{cond(roof)}=(T_{r,o}-T_{r,i})/R_r \tag{2.6}$$

Roof Inside Surface-Room Air Interface

As indicated in Figure 2.1, the heat transfer mechanisms acting at the inside surface are conduction, radiation, and convection.

$$q_{cond(roof)}=q_{rad(inside)}+q_{conv(inside)} \tag{2.7}$$

$$q_{rad(inside)}=\varepsilon\sigma(T_{r,i}^4-T_{set}^4) \tag{2.8}$$

$$q_{conv(inside)}=h_i(T_{r,i}-T_{set}) \tag{2.9}$$

On the basis of weather data from a database that includes solar radiation, ambient temperature, and humidity, the above equations can be solved iteratively to obtain a predicted roof surface temperature and a predicted conductive heat flux into the roof. This is based on Kondepudi's assumption [6] that there are no thermal capacitance effects of the roof or water film

Thermal Capacitance Effects of Roof

The above discussion provides a simple methodology for predicting the outside roof temperatures and heat fluxes if the thermal capacitance effects of the roof are neglected. In actual applications the thermal mass effects of the building envelope can play an important role in decreasing and/or shifting the phase of the cooling load on a building. Several load calculation methodologies have been developed to account for this thermal mass effect. Spitler and McQuiston [12] presented a review of the most popular cooling load calculation methodologies that are being used for manual and computer calculations. Because of the proliferation of computers in calculating cooling loads, The American Society of Heating, Refrigerating, and Air-Conditioning Engineers (ASHRAE) [13] is currently concentrating its research on improving and expanding the range of circumstances to which the TFM can be applied.

The TFM, as described by Mitalas [14], was developed in the late 1960's as a computer-oriented load calculation method that applies weighting

factors to the loads experienced by the exterior surfaces of a building to account for the thermal storage effects of the building envelope. These weighting factors are referred to as conduction transfer function (CTF) coefficients and relate the difference in the sol-air temperature and the inside space temperature to predict the difference in magnitude and phase shift between the load on the outside surface of the structure and the load that is converted to a cooling load. Sol-air temperature [13] is an equivalent outside air temperature that, in the absence of all radiation changes, accounts for the heat transferred to the exterior surface due to the combination of incident solar radiation and radiative and convective heat transfer between the exterior surface and the ambient air based on

$$T_e = T_a + \alpha q_{solar} / h_o - \varepsilon \delta R / h_o \qquad (2.10)$$

which is derived from the following two equations [13]:

$$q = \alpha q_{solar} + h_o (T_a - T_{r,o}) - \varepsilon \delta R \qquad (2.11)$$

$$q = h_o (T_e - T_{r,o}) \qquad (2.12)$$

Based on the sol-air temperature described above and a constant inside room air temperature, the TFM predicts the heat gain through a roof by the following equation.

$$q_{c,\theta}=\sum_{n=0} b_n(T_{c,\theta-n\delta})-\sum_{n=1} d_n(q_{c,\theta-n\delta})-T_{sa}\sum_{n=0} c_n \qquad (2.13)$$

The CTF coefficients take into account the heat transfer coefficients at the exterior and interior surfaces of the roof and the roof construction. CTF coefficients can be calculated using a computer program presented by McQuiston and Spitler [7] or use approximate values of CTF coefficients that were developed based on investigations by Harris and McQuiston [15] into the thermal characteristics of walls and roofs and their effect on the heat transfer to conditioned spaces. These approximate values are available in tabular form in various texts (see [7] and [13] , for instance) and are included in many computerized load calculation programs such as the software provided in Carrasco et al. [4] and the Load Design Program [16].

Combined Mathematical Model

The models for evaporative roof-spray cooling by Kondepudi [6] and the Transfer Function Method (TFM) described above were combined to predict the effect of evaporative roof-spray cooling and the thermal capacitance effect of roof construction. Due to the iterative nature of the solution of the roof-spray cooling problem and the application of the TFM, the use of a computer to solve the combined problem is virtually imperative. The problem is solved in a two-step process that first ignores the thermal capacitance effect of the roof to predict a heat flux into the roof and then

applies the TFM to predict the cooling load on the interior space that results from the calculated exterior heat flux. This solution predicts the amplitude decay in the load as a result of the evaporative cooling and the roof construction and the phase shift in the cooling load as a result of the thermal behavior of the roof in response to imposed loads.

Experimental Roof Parameters

The thermal characteristics of the roof that Somasundaram et al. [5] used in their experiments are provided in Table 2.1, which includes conduction transfer coefficients obtained from Reference [16]. The thermal properties of each layer were taken from measurements made by Somasundaram et al. [5] and from tabular data from Reference [13]. A study of the resulting amplitude decay and phase shift in the cooling load is conducted in Chapter 3.

Weather Model and Data

The weather data that was used for the prediction of heat transfer in the Bryan, Texas roof was taken from the Typical Meteorological Year (TMY) readings for Waco, Texas averaged over the period of the experimental roof-spray cooling. The data of Waco, Texas were used because it is located only 75 miles from Bryan, Texas, which has similar summer design temperatures, and it is only 70 meters higher in elevation [13]. The ASHRAE

solar heat flux calculation method [13] which is based on the work by Threlkeld and Jordan [17] could also be used. TMY weather tape was selected for its solar radiation data that makes it a good choice for solar design problems.

Actual experiment site weather measurements including ambient wet- and dry-bulb temperatures, solar radiation, and wind speed were reported by Houghten et al. [1] for the experiments in Pittsburgh. Ambient pressure data were extracted from Trane Typical Cooling Day weather files for Pittsburgh [16]. Typical Cooling Day pressure varied only 340 Pa, so a constant pressure could have been assumed with little effect on predicted results.

Table 2.1: Thermal Characteristics of Roof at Bryan, Texas

Description	Physical Description				
	Thickness {mm}	Conductivity {W/m² F}	Density {kg/m³}	Specific Heat {kJ/(kg K)}	Resistance {(m² K)/W}
Outside air film	0	.000	0	.00	.044
Rigid insulation	25	.043	32	.84	.587
Felt and asphalt	10	.192	1121	1.68	.050
Gypsum roof deck	150	.156	800	1.09	.978
Mineral insulation	150	.069	10	.84	2.201
Insulation air film	0	.000	0	.00	.120

Decrement factor = .120, Overall weight = 135 kg/m² , Overall U-value = .250 W/(m² K)
Time delay = 11 Hours, Heat capacity = 337 kJ/(m² kg K), C_n coefficient = .183E-02

n	B_n coefficients	D_n coefficients
0	.1733146E-08	.1000000E+01
1	.1402007E-04	-.2086841E+01
2	.3365204E-03	.1422010E+01
3	.9128446E-03	-.3563488E+00
4	.5027138E-03	.2923254E-01
5	.6378616E-04	-.7691044E-03
6	.1774670E-05	.5973486E-05

Table 2.2: Thermal Characteristics of 50 mm Thick Concrete Roof at Pittsburgh

Physical Description

Description	Thickness {mm}	Conductivity {W/m^2 K}	Density {kg/m^3}	Specific Heat {kJ/(kg K)}	Resistance {(m^2 K)/W}
Outside air film	0	.000	0	.00	.044
Slag	13	1.436	880	1.68	.009
Felt and asphalt	10	.192	1120	1.68	.050
Slag	13	1.436	880	1.68	.009
Felt and Asphalt	19	.192	1120	1.68	.050
Concrete	50	1.731	2240	.84	.029
Inside air film	0	.000	0	.00	.120

Decrement factor = .775, Overall weight = 168 kg/m^2, Overall U-value = .346 W/(m^2 K)
Time delay = 4 Hours, Heat capacity = 410 kJ/(m^2 kg K), C_n coefficient = .653

n	B_n coefficients	D_n coefficients
0	.3732012E-01	.1000000E+01
1	.3805050E+01	-.9006944E+00
2	.2269784E+00	.1360358E+00
3	.9101764E-02	-.2234380E-03
4	.7930927E-05	.5431017E-08
5	.8646022E-11	0
6	0	0

Table 2.3: Thermal Characteristics of 50 mm Thick Pine Plank Roof at Pittsburgh

Physical Description

Description	Thickness {mm}	Conductivity {W/m² F}	Density {kg/m³}	Specific Heat {kJ/(kg K)}	Resistance {(m² K)/W}
Outside air film	0	.000	0	.00	.044
Slag	13	1.436	880	1.68	.009
Felt and asphalt	10	.192	1120	1.68	.050
Slag	13	1.436	880	1.68	.009
Felt and Asphalt	19	.192	1120	1.68	.050
Pine Planking	50	.121	590	2.51	.419
Inside air film	0	.000	0	.00	.120

Decrement factor = .708, Overall weight = 84 kg/m², Overall U-value = 1.33 W/(m² K)
Time delay = 5 Hours, Heat capacity = 370 kJ/(m² kg K), C_n coefficient = .189

n	B_n coefficients	D_n coefficients
0	.3732012E-01	.1000000E+01
1	.3805050E+01	-.9006944E+00
2	.2269784E+00	.1360358E+00
3	.9101764E-02	-.2234380E-03
4	.7930927E-05	.5431017E-08
5	.8646022E-11	0
6	0	0

CHAPTER 3
RESULTS

Introduction

This section presents the numerical results of predicted cooling loads along with the experimental results. First, the predicted results for a structure in Bryan, Texas are compared to the experimental results obtained by Somasundaram and Carrasco [5]. Then predicted cooling loads for two roofs at Pittsburgh are compared to experimental results of Houghten et al. [1].

Roof Heat Transfer and Temperatures at Bryan, Texas

The comparisons of the experimental data and numerical predictions for the roof-spray cooled roof at Bryan, Texas are plotted in Figures 3.1 and 3.2 and provided in Table 3.1. The predicted average heat gain through the roof, q_e, of -4.7 $\pm$1.2 W/m^2 is in very good agreement with the experimental value of -4.2 W/m^2. The predicted outside roof surface temperatures are in good agreement with the experimental data, with an average overprediction of less than one °C. The peak predicted conductive heat flux through the outside of the roof, $q_{cond(roof)}$, is lower than the peak experimental data. The average predicted $q_{cond(roof)}$ is 90% higher than the experimental results. Some

variations are expected due to the thermal capacitance effects of the roof that were neglected in the prediction of the outer conductive heat flux and the fact that the outside flux meter was located below the gypsum roof deck in the experiments.

The results plotted in Figures 3.1 and 3.2 also indicate two likely problem areas with the models used to predict results. These are weather and the thermal properties of the roof. First, although the cumulative daily solar radiation obtained from the TMY weather data [17] is very near the experimental amount, Table 3.2, the peak experimental solar radiation was likely higher at midday and tapered off more rapidly at times other than midday. This would account, in part, for the differences in the shapes of the predicted and experimental outside surface heat flux and temperature curves. The second likely weather problem was an underprediction of the net nocturnal radiation exchange between the roof and the atmosphere that was reflected in the underprediction of the nighttime cooling effect. This also would have contributed to the predicted average $q_{cond(roof)}$ being 90% higher than the experimental average value. Minor inaccuracies in the thermal properties of the roof model including the convective heat transfer coefficients also would have contributed to some of the differences in the experimental and predicted results. This can be illustrated by the fact that the predicted difference between the maximum and minimum values of q_e is 0.7 W/m^2 while

the experimental difference is 1.6 W/m^2 which may be a result of inaccuracies in the mass and thermal conductivity of the roof materials used in the mathematical model of the roof provided in Table 2.1.

As a check on the validity of the roof and exterior load models, experimental results from dry, no roof-spray cooling, tests on the same roof during the period of 17-21 August were compared to predicted results. The comparison of experimental data and numerical predictions for the dry roof are plotted in Figures 3.3 and 3.4. Due to the 21% difference in experimental and TMY cumulative solar radiation data, the TMY hourly solar radiation data were adjusted upward to match the experimental daily cumulative data. The TMY hourly ambient temperatures averaged only 1.1 °C lower than the experimental data and were not adjusted.

The predicted difference between the maximum and minimum values of q_e is 1.2 W/m^2 while the experimental difference is 1.3 W/m^2 which indicates a good representation of the thermal capacitance effects of the roof. The predicted average q_e of 2.4 ± 1 W/m^2 is in moderately good agreement with the experimental value of 0.8 W/m^2. This difference may be a result of a combination of inaccuracies in the weather, heat transfer model, and thermal characteristics of the roof that are magnified by the higher heat fluxes associated with the dry roof condition.

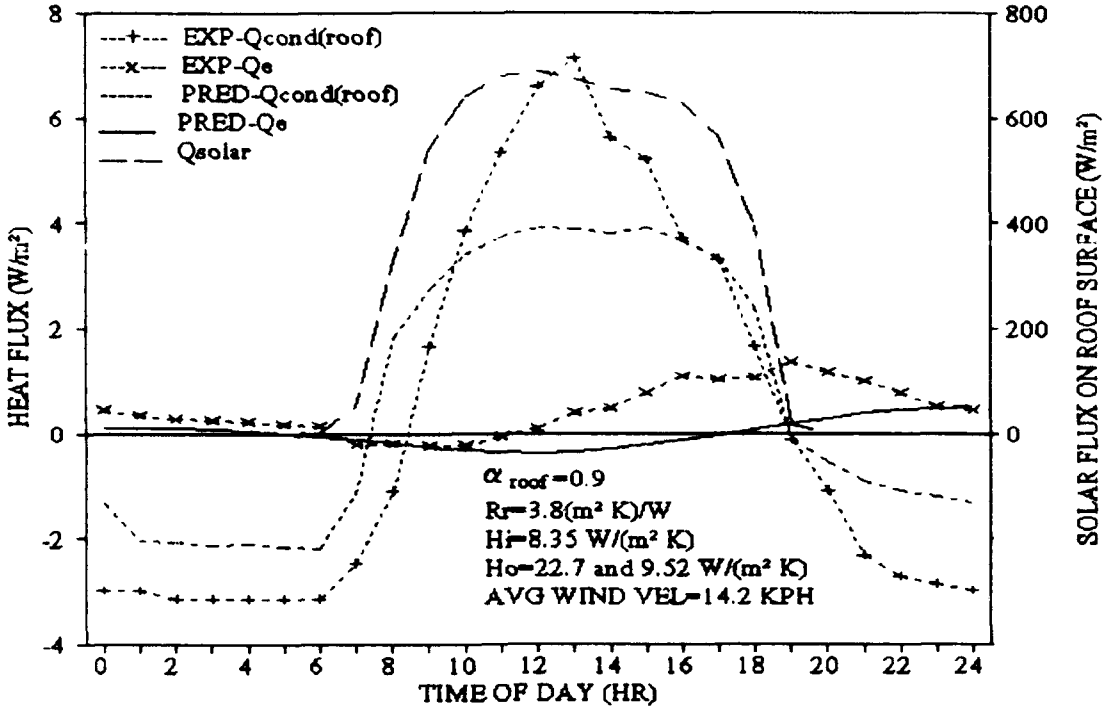

Figure 3.1: Relation Between Time and Heat Flux Trough Outside and Inside Surfaces of Roof-Spray Cooled Roof at Bryan, Texas, in July

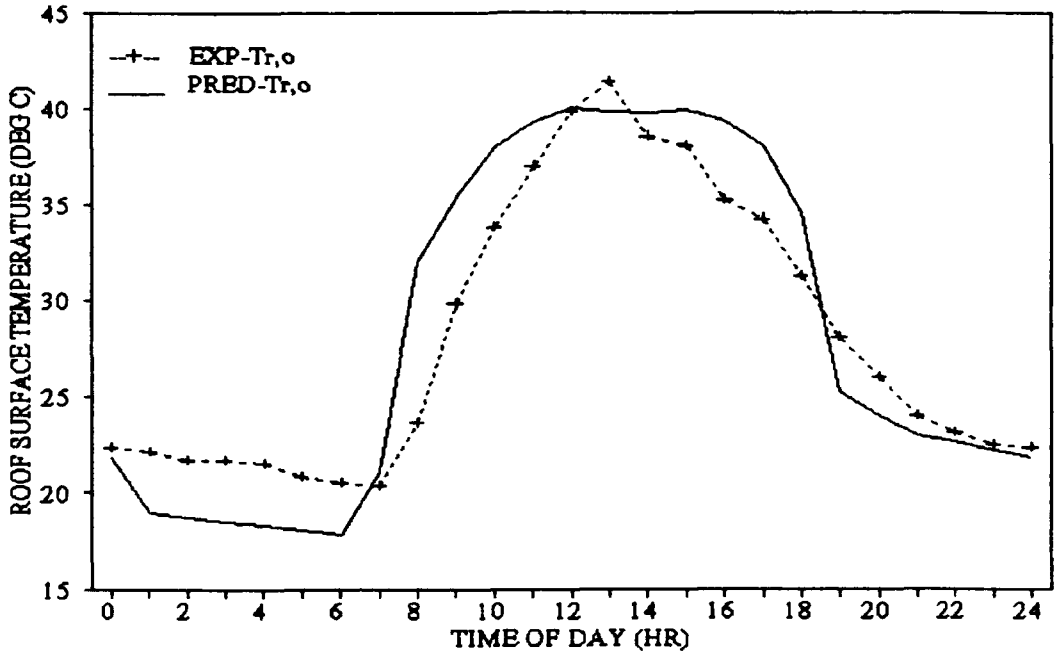

Figure 3.2: Relation Between Time and Temperature of Outside Surface of Roof-Spray Cooled Roof at Bryan, Texas, in July

Table 3.1: Experimental and Predicted Heat Flux and Temperature Comparison for Roof-Spray Cooled Roof at Bryan, Texas

	July 17 - July 30, 1987			
	Outside surface		Inside surface	
	Experimental	Predicted	Experimental	Predicted
Average Roof Heat Flux (W/m^2)	0.40	0.76	0.44	0.40 $\pm$0.2
Maximum and Minimum Roof Heat Flux (W/m^2)	7.1 -3.1	3.9 -2.1	1.3 -0.2	0.8 0.1
Cumulative Daily Roof Heat Flux ($W\ h/m^2$)	9.5	18.3	10.5	10.0
Average Roof Surface Temperature (°C)	28.2	29.1	26.7	Note:1
Maximum and Minimum Roof Surface Temperature (°C)	41.4 20.3	41.2 18.8	27.7 25.8	Note:1 Note:1

Note: 1. Experimental data for inside surface temperature were used in the predict other table values.

Source: Experimental data from reference [5].

Table 3.2 Experimental and Predicted Weather for Bryan, Texas, and Pittsburgh

	Bryan, Texas				Pittsburgh
	Wet Roof Test Date		Dry Roof Test Date		Wet Roof Test Date
	July 17-July 30		August 17-August 21		8 September-9 September
	Experimental	Predicted	Experimental	Predicted	Experimental
Cumulative Daily Solar Radiation ($W\ hr/m^2$ /24 hrs)	6398	6497	6492	5114 Note:1	3613
Average Ambient Temperature (°C)	28.54	28.64	30.24	29.12	26.3
Maximum and Minimum Ambient Temperatures (°C)	34.79 23.12	34.44 22.72	37.49 24.33	33.89 25.00	35.0 18.6
Average Wind Speed (k/hr)	Note: 2	14.2	Note: 2	13.6	22.3
Maximum and Minimum Hourly Average Wind Speed (k/hr)	Note: 2 Note: 2	17.8 10.2	Note: 2 Note: 2	16.7 10.6	38.6 9.7

Notes: 1. Due to large difference between predicted and experimental values, solar data were adjusted to experimental value for predicting other table values.
2. No experimental wind data available.

Sources: Experimental data from Reference [5].
Predicted data from Reference [17].

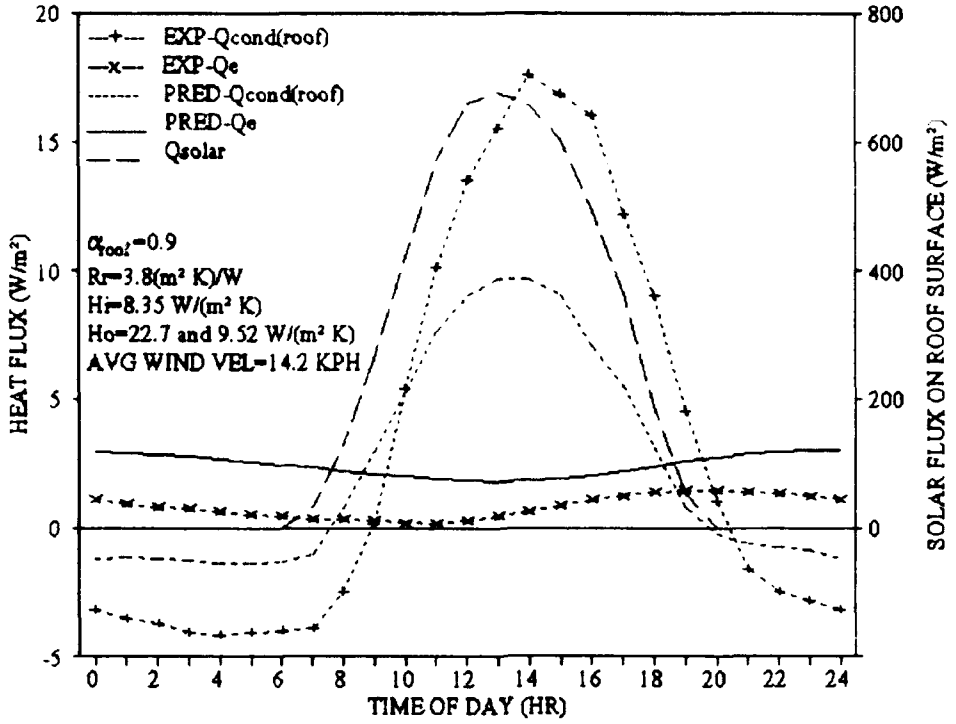

Figure 3.3: Relation Between Time and Heat Flux Trough Outside and Inside Surfaces of Dry Roof at Bryan, Texas, in July

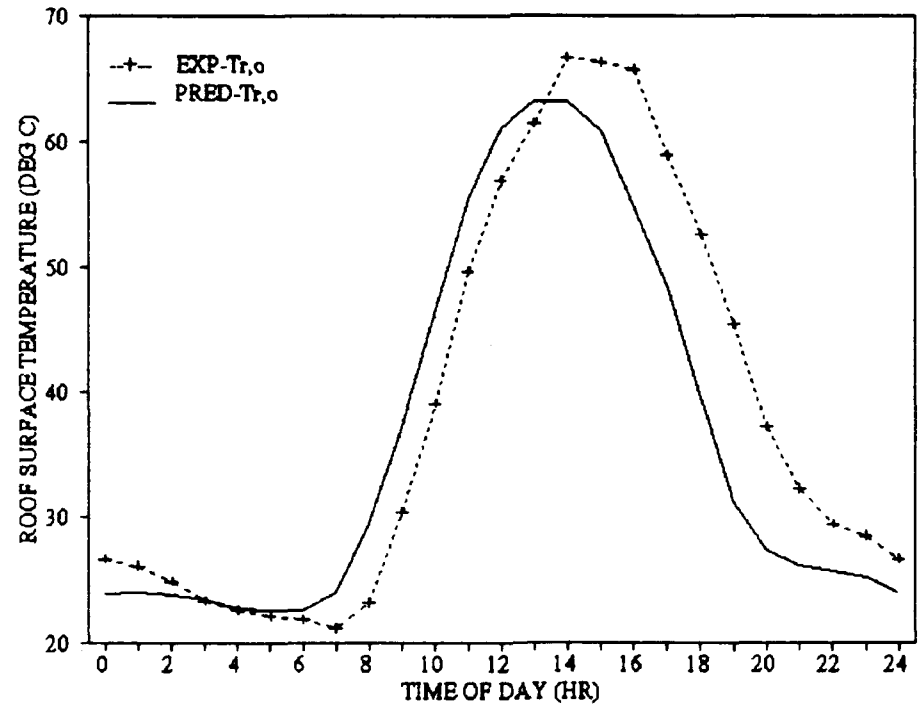

Figure 3.4: Relation Between Time and Temperature of Outside Surface of Dry Roof at Bryan, Texas, in July

Table 3.3: Experimental and Predicted Heat Flux and Temperature Comparison for Dry Roof at Bryan, Texas

	August 17 - August 21, 1987			
	Outside surface		Inside surface	
	Experimental	Predicted	Experimental	Predicted
Average Roof Heat Flux (W/m^2)	3.4	2.4	0.8	2.4 ±1.0
Maximum and Minimum Roof Heat Flux (W/m^2)	17.6 -4.1	9.7 -1.4	1.5 0.2	3.0 1.8
Cumulative Daily Roof Heat Flux ($W\ h/m^2$)	82.5	58.5	19.3	58.2
Average Roof Surface Temperature (°C)	38.8	37.2	28.3	Note:1
Maximum and Minimum Roof Surface Temperature (°C)	66.7 21.1	63.6 23.1	29.4 26.9	Note:1 Note:1

Note: 1. Experimental data for inside surface temperature was used in the prediction of other table values.

Source: Experimental data from reference [5].

Roof Heat Transfer at Pittsburgh

The numerical predictions and experimental data for the concrete roof, which are given in Table 3.4 and in Figure 3.5, show good agreement. No experimental outside roof heat flux or temperature data are available. However, the experimental and predicted inside heat flux for the concrete roof

are in good agreement in hourly magnitude, phase shift, and cumulative daily heat flux into the room. The predicted average q_e of -4.7 $\pm$1.2 W/m^2 is in very good agreement with the experimental value of -4.2 W/m^2. The predicted difference between the maximum and minimum values of q_e is 28.2 W/m^2, 34% higher than the experimental difference, 21.1 W/m^2. The differences in the predicted and experimental inside heat fluxes may, in part, be attributed to minor inaccuracies in the mathematical descriptions of the roof and the models of heat transfer at the roof surfaces.

The numerical predictions and experimental data for the pine plank roof, which are given in Table 3.5 and in Figure 3.6, show moderately good agreement. The average predicted q_e of -4.2 $\pm$1.4 W/m^2 is in moderately good agreement with the experimental value of -2.6 W/m^2. The difference between the predicted and experimental values and the approximate two hour difference in the phases of the predicted and experimental q_e indicate that the mathematical description of the pine plank roof is inaccurate. The mathematical descriptions of the Pittsburgh roofs are based on sketches by Houghten et al. [1] that provide no thermal characteristics of the roof materials. There is a large uncertainty in the thermal response modeling of the pine plank roof because of the unknown characteristics of the pine planking. It is unknown if the two inch thickness of the pine planking given by Houghten is the actual or nominal thickness. Also, the density, thermal conductivity, and specific heat of the wood could vary by over 30% depending on the

specific species and moisture content of the planking. An example of the variation in the thermal properties of a material from expected is the thermal conductivity of the Bryan, Texas mineral insulation that testing [5] revealed was 60% higher than values found in Reference [9].

Summary

The computer code, based on the mathematical models, provides a moderate to good comparison with experimental results of heat flux through the inside surface of a roof and into a room. The predicted average heat gain through the roof for the Bryan, Texas insulated concrete roof, the Pittsburgh concrete roof, and Pittsburgh pine plank roof are in good agreement with the experimental averages. The prediction of heat flux and temperature at the outside surface of the roof provided good qualitative comparison with experimental results. However, large magnitude and small phase differences from experimental data were obtained as a result of the thermal capacitance effects of the roof that were neglected in the prediction of the outside surface temperature and heat flux and the placement of the outside roof heat flux meter below the gypsum decking.

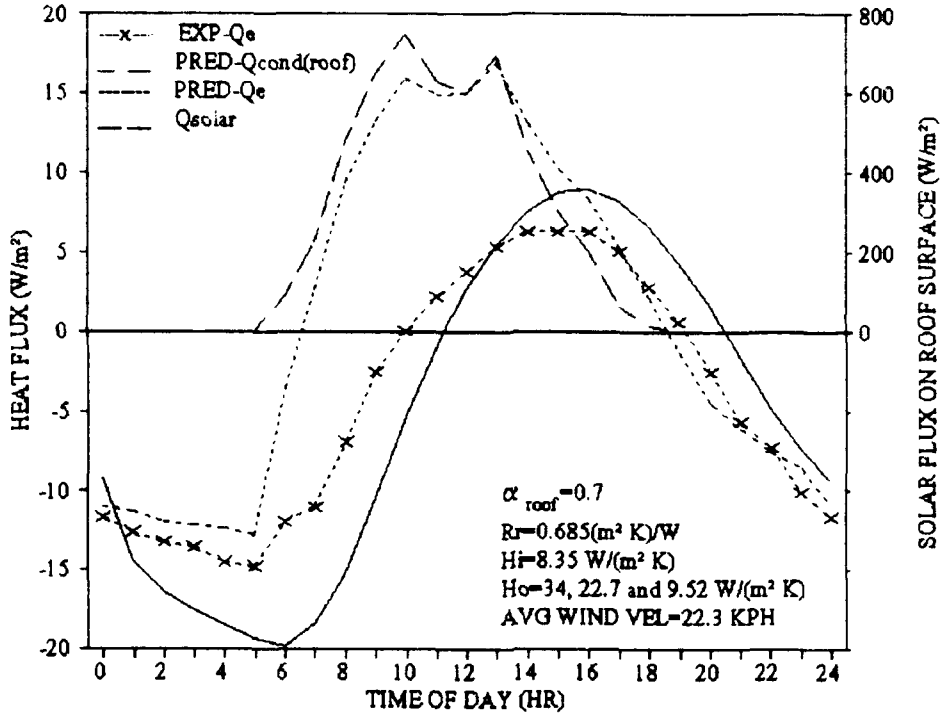

Figure 3.5: Relation Between Time and Heat Flux Through Outside and Inside Surfaces of Concrete Roof at Pittsburgh

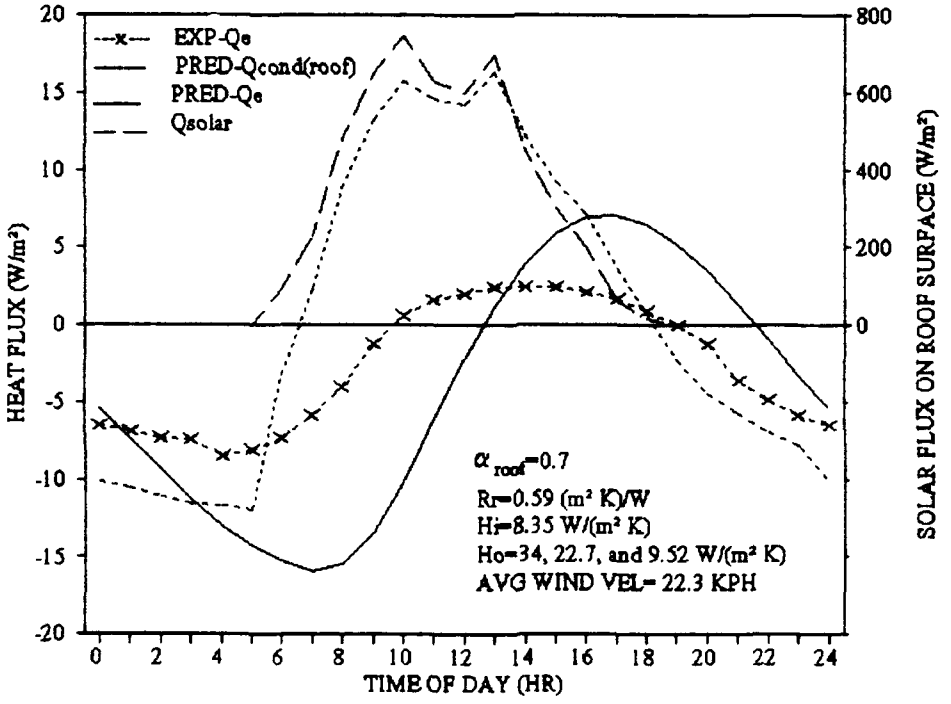

Figure 3.6: Relation Between Time and Heat Flux Through Outside and Inside Surfaces of Pine Plank Roof at Pittsburgh

Table 3.4: Experimental and Predicted Heat Flux Comparison for Roof-Spray Cooled Concrete Roof at Pittsburgh

	August 8, 1939		
	Outside surface	Inside surface	
	Predicted	Experimental	Predicted
Average Roof Heat Flux (W/m^2)	1.0	-4.2	-4.7 $\pm$1.2
Maximum and Minimum Roof Heat Flux (W/m^2)	15.6 -12.9	6.3 -14.8	9.1 -19.1
Cumulative Daily Roof Heat Flux (W h/m2)	24.6	-99.5	-113.5

Source: Experimental data from reference [1].

Table 3.5: Experimental and Predicted Heat Flux Comparison for Roof-Spray Cooled Pine Plank Roof at Pittsburgh

	August 8, 1939		
	Outside surface	Inside surface	
	Predicted	Experimental	Predicted
Average Roof Heat Flux (W/m^2)	0.9	-2.6	-4.2 $\pm$1.4
Maximum and Minimum Roof Heat Flux (W/m^2)	16.4 -11.9	2.4 -8.5	7.1 -15.9
Cumulative Daily Roof Heat Flux (Wh/m^2)	21.2	-62.3	-101.7

Source: Experimental data from reference [1].

CHAPTER 4
CONCLUSIONS AND RECOMMENDATIONS

Conclusions

The objective of this thesis was to combine existing models for evaporative roof-spray cooling and the transient heat flow through roofs to provide a model that will predict roof cooling loads based on known weather data and roof material descriptions. The best evaluation of the effectiveness of the model is by comparison to well-documented experimental data.

Two roof conditions were studied. One was dry roof (no spray cooling), and the other was damp roof (spray cooled). Three different roof constructions at two locations were studied. The roofs included an insulated gypsum deck, an uninsulated concrete deck, and an uninsulated pine plank deck.

The mathematical formulation gave a simple but effective prediction of the roof cooling load for an interior that is maintained at a fairly constant temperature. The agreement of experimental data with predictions of roof cooling loads as a result of the combined effects of roof-spray cooling and roof construction gave a high level of confidence that the use of the combined roof-spray cooling and Transfer Function Method model will yield good

predictions for buildings maintained at a constant internal temperature. The agreement between predicted and experimental average heat gain through the roof, q_e, values was very good making the predicted values a useful tool in predicting the energy usage for roof-spray cooled buildings.

The uncertainty analysis described in Appendix B indicate that the thermal characteristics of the composite roof are important factors in dry and damp roof cooling load calculations and must be accurately described to ensure the accuracy of the predicted heat gains through the roof . Two other variables that have a large affect on the uncertainty of the predicted heat gain are the external convective heat transfer coefficient, h_o, and the solar radiation transferred to the roof surface as a result of the incident solar radiation and the absorptance of the surface of the roof. Since h_o is largely a function of the wind speed across the roof, accurate measurement of the wind speed at the building location is important to allow the accurate prediction of h_o. The effect of changes in the absorptance of the roof surface indicates the importance of this measurement to allow the accurate prediction of solar radiation transferred to the roof. It also indicates the value of low absorptance roof surfaces for dry and roof-spray cooled buildings. The need to accurately measure the wind speed and incident solar radiation is important, not only for experimental activities, but for use in the prediction of the required application of water to the roof surface. Therefore the installation of

anemometric and heliopyrometric devices as part of the roof-spray cooling system may be desirable for the optimization of roof sprays for larger buildings.

Recommendations

The following is a list of suggested improvements that can be included in the modeling of roof-spray cooled structures.

1) The variation in wind speed over the roof can be incorporated into the convective heat transfer portion of the outside load calculation.

2) The effect of variations in cloud cover and sky clearness on the net radiative heat exchange between the roof and the atmosphere can be included in the outside load calculation.

3) The predicted evaporative heat transfer rates can be extended to predict the variation in the required rate of delivery of water to the roof to optimize the cooling effect without the application of excess water.

4) Various roof surface materials such as aggregate ballast of different sizes and colors can be compared to smooth roof surfaces to determine any effects on the heat transfer at the roof surface.

The mathematical formulation provided acceptable results for buildings maintained at constant inside temperatures. The validation of this model for

buildings that are maintained at different temperatures during a daily or weekly cycle is needed because of the common usage of temperature setbacks as an energy conservation measure.

Any further experiments on roof-spray cooling should include a study of the roof's thermal properties including surface absorptivities and emissivities in addition to ambient weather conditions that include dry-bulb temperature, humidity, wind speed, pressure, solar radiation, cloud cover, and precipitation.

APPENDIX A
COMPUTER CODE LISTING

This section includes the BASIC computer code that was used to calculate the predicted heat fluxes at the exterior and interior surfaces of the roof with roof-spray cooling in Bryan, Texas. Although the code includes the data for many input parameters in the text, the code could be easily modified to read these parameters from an input data file or to prompt the user for the input values. The code could also be easily translated into FORTRAN if desired for compatibility with other software or data files.

The following code calculates the predicted heat fluxes at the exterior and interior roof surfaces of a test building that Somasundaram et al. [3] used for roof-spray cooling experiments. In this example combined convective and radiative heat transfer coefficients were used, but the code allows the use of convective-only heat transfer coefficients if the radiative heat fluxes are not set equal to zero. The external convective heat transfer coefficient, h_o, can also be varied if needed to account for large variations in wind speed, v.

The iterative techniques used in this code proved to be effective in the required simulation. However, the speed of the solution could be improved through the application of more sophisticated bracketing and convergence techniques.

```
      REM  ROOF-SPRAY COOLED ROOF AT BRYAN, TEXAS (IN FILE
           ATMYBRTX.BAS)
      REM  HEAT FLOW CALCULATION BY TRANSFER FUNCTION
           METHOD
      OPEN "C:ATMBRTX.PRN" FOR OUTPUT AS #1
      WRITE #1, "Hour", "OMEGA", "Tset", "Ta", "Twet", "TrO", "Try",
           "Qsolar", "Qevap", "QcondO", "Qe", "QoutEXP", "QinEXP",
           "qCONVo", "pWR", "pW", " "
      LET T=0
    5 LET H=T
    6 IF H>=24 THEN H=H-24
      IF H>=24 GOTO 6
      DIM Tr(-6 TO 120), TE(-6 TO 120), QE(-6 TO 120), Try(-6 TO 120),
           I(0 TO 120), QEXPout(0 TO 120), QEXPin(0 TO 120)
      REM  Tdry-bulb, Twet-bulb, PRESSURE, HUMIDITY, AND SOLAR
           VALUES FROM TYPICAL METEOROLOGICAL YEAR
           WEATHER DATA AVERAGED FOR PERIOD 17-30 JULY FOR
           WACO, TEXAS
      REM  WEATHER FILES OBTAINED FROM ACROSOFT
           INTERNATIONAL, INC., DENVER, CO AND PROCESSED BY
           MICRO-DOE2 SOFTWARE
REM   EXPERIMENTAL DATA FROM SOMASUNDARAM et al. [1988] pp.
           1103-1104
      IF H=0 THEN TW=69: TAMB=79.3: P=29.45: W=.031: QSOL=0:
           QEXPout=-3: QEXPin=.45
      IF H=1 THEN TW=69: TAMB=77.8: P=29.47: W=.0136: QSOL=0:
           QEXPout=-3: QEXPin=.34
      IF H=2 THEN TW=68.9: TAMB=76.5: P=29.47: W=.0138: QSOL=0:
           QEXPout=-3.15: QEXPin=.27
      IF H=3 THEN TW=68.7: TAMB=75.3: P=29.47: W=.014: QSOL=0:
           QEXPout=-3.15: QEXPin=.24
      IF H=4 THEN TW=68.6. TAMB=74.6: P=29.48: W=.014: QSOL=0:
           QEXPout=-3.15: QEXPin=.21
      IF H=5 THEN TW=68.3: TAMB=73.7: P=29.48: W=.014: QSOL=0:
           QEXPout=-3.15: QEXPin=.17
      IF H=6 THEN TW=68.1: TAMB=72.9: P=29.49: W=.014: QSOL=0:
           QEXPout=-3.15: QEXPin=.14
      IF H=7 THEN TW=69.7: TAMB=76: P=29.51: W=.0145: QSOL=15.5:
           QEXPout=-2.47: QEXPin=-.21
      IF H=8 THEN TW=71.1: TAMB=79.1: P=29.51: W=.0149:
           QSOL=104.9: QEXPout=-1.1: QEXPin=-.2
```

```
IF H=9 THEN TW=72.6: TAMB=82.2: P=29.51: W=.0153:
      QSOL=170.3: QEXPout=1.64: QEXPin=-.24
IF H=10 THEN TW=72.7: TAMB=84.9: P=29.51: W=.0149:
      QSOL=202.6: QEXPout=3.83: QEXPin=-.24
IF H=11 THEN TW=73.1: TAMB=87.4: P=29.51: W=.0146:
      QSOL=215.4: QEXPout=5.34: QEXPin=-.07
IF H=12 THEN TW=73.3: TAMB=90.1: P=29.49: W=.0141:
      QSOL=218.2: QEXPout=6.59: QEXPin=.09
IF H=13 THEN TW=73.1: TAMB=91.3: P=29.49: W=.0136:
      QSOL=213.1: QEXPout=7.12: QEXPin=.38
IF H=14 THEN TW=72.9: TAMB=92.7: P=29.47: W=.0132:
      QSOL=206.9: QEXPout=5.62: QEXPin=.48
IF H=15 THEN TW=72.9: TAMB=94: P=29.43: W=.0129:
      QSOL=205.4: QEXPout=5.2: QEXPin=.75
IF H=16 THEN TW=72.5: TAMB=93.3: P=29.41: W=.0128:
      QSOL=199.1: QEXPout=3.7: QEXPin=1.09
IF H=17 THEN TW=72.1: TAMB=92.7: P=29.41: W=.0126:
      QSOL=178.7: QEXPout=3.3: QEXPin=1.06
IF H=18 THEN TW=71.5: TAMB=92: P=29.41: W=.0122:
      QSOL=124.2: QEXPout=1.64: QEXPin=1.06
IF H=19 THEN TW=70.8: TAMB=88.7: P=29.41: W=.0124:
      QSOL=4.7: QEXPout=-.13: QEXPin=1.35
IF H=20 THEN TW=70.3: TAMB=85.9: P=29.42: W=.0127: QSOL=0:
      QEXPout=-1.1: QEXPin=1.16
IF H=21 THEN TW=69.8: TAMB=82.8: P=29.43: W=.0129: QSOL=0:
      QEXPout=-2.33: QEXPin=.99
IF H=22 THEN TW=69.5: TAMB=81.7: P=29.44: W=.0131: QSOL=0:
      QEXPout=-2.74: QEXPin=.75
IF H=23 THEN TW=69.1: TAMB=80.4: P=29.45: W=.0130: QSOL=0:
      QEXPout=-2.86: QEXPin=.49
IF H=24 THEN TW=69: TAMB=79.3: P=29.45: W=.031: QSOL=0:
      QEXPout=-3: QEXPin=.45
REM  END OF TMY DATA
P=P*3386.4: REM CONVERT PRESSURE FROM INCHES HG TO Pa
Pw=(P*W)/(.62198+W): REM CALCULATE PARTIAL PRESSURE OF
      WATER IN MOIST AMBIENT AIR
LET QSOL=.6*QSOL*3.155: REM APPLY ROOF ABSORPTANCE
      AND CONVERT FROM Btuh/sf TO W/m**2
Twet=(TW-32)/1.8+273.15: REM CONVERT WET BULB TEMP
      FROM F TO K
TAMB=(TAMB-32)/1.8+273.15: REM CONVERT DRY BULB TEMP
      FROM F TO K
```

```
      REM  FROM ROOF GROUP #166 BUILD ON TRANE TRACE 600
           ROOF GENERATOR UTILITY BASED ON SOMASUNDARAM
           et al. TEST BUILDING
      REM  DESCRIPTION OF ROOF, CONDUCTION TRANSFER
           FUNCTION COEFFICIENTS
      B0 = 4.40399E-09*5.6783: REM CONVERT Bn AND Cn TO SI UNIT
      B1 = 1.461269E-05*5.6783: B2 = 2.489753E-04*5.6783
      B3 = 5.109677E-04*5.6783: B4 = 2.08079E-04*5.6783
      B5 = 1.789627E-05*5.6783: B6 = 2.828292E-07*5.6783
      Cn = .001*5.6783: D0 = 1
      D1 = -1.974663: D2 = 1.273348: D3 = -.3056189
      D4 = .02383278: D5 = -4.312459E-04: D6 = 1.107164E-06
      REM TIME LAG = 9 HOURS, Utable = .061*5.6783, W/(m**2*K)
      REM DF = .227, DECREMENT FACTOR, AMPLITUDE REDUCTION
           FACTOR FROM OUTSIDE HEAT FLUX TO INTERIOR LOAD
      Ho = 22.7: REM EXT CONVECTIVE AND RADIATIVE HEAT
           TRANSFER COEFFICIENT, W/(m**2*K)
      Hi = 8.35: REM INT CONVECTIVE AND RADIATIVE HEAT
           TRANSFER COEFFICIENT, W/(m**2*K)
      EPS = .85: REM EMISSIVITY OF ROOF
      SIG = 5.67E-08: REM STEFAN-BOLTZMAN CONSTANT,
           W/(m**2*K**4)
      Rr = 2.079: REM THERMAL RESISTANCE OF ROOF, m**2*K/W
      TSET = 299.81: REM AMBIENT TEMPERATURE OF INSIDE AIR
           PLENUM, K
      LET Try(-1) = 280: REM PROVIDES STARTING TRIAL TEMP FOR
           HOUR 0
      IF T>=24 THEN Try(T)=Try(T-24)- 1.0001: GOTO 20
      Try(T) = Try(T-1) - 20
20    Fry = Try(T)*1.8: CONVERT TEMP FROM K TO F
      REM CALCULATE SATURATION PRESSURE OF WATER ON
           ROOF SURFACE FROM MATHUR [1988]
      PART0 = 670.2012: PART1 = -5.325521*Fry
      PART2 = .0159464*Fry**2: PART3 = -.00002134061*Fry**3
      PART4 = 1.077853E-08*Fry**4
      Pwr = (PART0+PART1+PART2+PART3+PART4)*6894.8: REM Pa
      QEVAP = .073814*(Pwr-Pw): REM CALCULATE EVAPORATIVE
           HEAT TRANSFER DUE TO PRESSURE DIFFERENCE OF
           WATER VAPOR AT ROOF SURFACE AND IN AMBIENT AIR
      REM Tr(T) = TAMB+Rr*(-QEVAP-QRAD-QCONV+QSOL)
      QRADo = EPS*SIG*(Try(T)**4-(TAMB-3)**4)
      QCONVo = Ho*(Try(T)-TAMB)
```

```
      Tri = Try(T)+Rr*(QRADo+QEVAP+QCONVo-QSOL): REM CALC
            INT ROOF TEMP, K
      QCONDo = -QRADO-QEVAP-QCONVo+QSOL
      QCONVi = Hi*(Tri-TSET)
      QRADi = EPS*SIG*(Tri**4-TSET**4)
      REM QCONDi = QCONVi=QRADi: REM INT SURFACE ENERGY
            BALANCE
      Tr(T) = Tri+Rr*(QCONVi+QRADi)
      IF ABS(Tr(T)-Try(T))<.1 GOTO 40: REM CHECK FOR
            CONVERGENCE OF TRIAL ROOF TEMP WITH
            CALCULATED TEMPERATURE
      REM SET  STEP SIZE TO CALCULATE OUTSIDE ROOF  TEMP
      IF Tr(T)>285 AND Tri>0 THEN I(T)=.0001: GOTO 30
      IF Tr(T)>270 AND Tri>0 THEN I(T)=.001: GOTO 30
      IF Tr(T)>0 AND Tri>0 THEN I(T)=.01: GOTO 30
      IF Tr(T)<0 OR Tri<0 THEN I(T)=.1
30    LET Try(T) = Try(T)+I(T): REM ADD ITERATIVE STEP TO
            PREVIOUS TRIAL ROOF TEMPERATURE
      IF Try(T)>Tr(T-1)+20 THEN PRINT "ERROR ON ITERATIVE
            LOOP": GOTO 50
      GOTO 20
40    REM SOL-AIR TEMPERATURE WILL BE TAKEN AS
            CALCULATED ROOF SURFACE TEMPERATURE
      LET TE(T) = Tr(T)-273.15: REM CONVERT ROOF TEMP FROM K
            TO C
      REM CALCULATE PREDICTED LOAD ON INTERIOR FROM ROOF
            BY TRANSFER FUNCTION METHOD
      QE1=B0*TE(T)+B1*TE(T-1)+B2*TE(T-2)+B3*TE(T-3)
      QE3=B4*TE(T-4)+B5*TE(T-5)+B6*TE(T-6)
      QE3=D1*QE(T-1)+D2*QE(T-2)+D3*QE(T-3)
      QE4=D4*QE(T-4)+D5*QE(T-5)+D6*QE(T-6)+(TSET-273.15)*Cn
      QE(T) = QE1+QE2-QE3-QE4
      REM WRITE OUTPUT DATA TO FILE
      WRITE #1, T, W, TSET, TAMB, TWET, Tr(T), QSOL, QEVAP,
            QCONDo, QE(T), QEXPout(T), QEXPin(T), QCONVo, Pwr, Pw
      LET T = T+1: REM START NEXT HOUR SIMULATION
      IF T>120.5 GOTO 50: REM STOP SIMULATION AFTER 120 HOURS
      GOTO 5
50    REM END OF WHILE LOOP
      CLOSE #1: REM CLOSE OUTPUT FILE ATMYBRTX.PRN
      END
```

```
      REM *********NOMENCLATURE*******************************
Bn        = CONDUCTION TRANSFER FUNCTION COEFFICIENTS
Cn        = CONDUCTION TRANSFER FUNCTION COEFFICIENTS
Dn        = CONDUCTION TRANSFER FUNCTION COEFFICIENTS
EPS       = EMISSIVITY
Fry       = TRIAL ROOF TEMPERATURE, DEGREES R
H         = HOUR OF DAY, MODULUS 24 CLOCK, HOURS
Hi        = INTERNAL CONVECTIVE(/ RADIATIVE) HEAT TRANSFER
              COEFFICIENT, W/(M**2*K)
Ho        = EXTERNAL CONVECTIVE(/ RADIATIVE) HEAT TRANSFER
              COEFFICIENT, W/(M**2*K)
P         = TOTAL PRESSURE OF MOIST AIR, INCHES HG, PSIA OR Pa
Pw        = PARTIAL PRESSURE OF WATER IN MOIST AIR, Pa
Pwr       = PARTIAL PRESSURE OF WATER AT ROOF SURFACE (Psat
              AT Troof), Pa
Rr        = THERMAL RESISTANCE OF ROOF, m**2*K/W
QCONDo = CONDUCTIVE HEAT FLUX INTO ROOF FROM OUTER
              SURFACE, W/m**2
QCONVi  = CONVECTIVE HEAT FLUX AT BOTTOM OF ROOF TO
              ROOM, W/m**2
QCONVo = CONVECTIVE HEAT FLUX AT TOP ROOF TO AMBIENT,
              W/m**2
QE(T)     = PREDICTED HEAT FLUX INTO ROOM, W/m**2
QEVAP     = EVAPORATIVE HEAT FLUX FROM MOIST ROOF, W/m**2
QRADi     = RADIATIVE HEAT TRANSFER FROM ROOF INNER
              SURFACE TO AMBIENT ROOM, W/m**2
QRADo     = RADIATIVE HEAT TRANSFER FROM ROOF OUTER
              SURFACE TO AMBIENT, W/m**2
QSOL      = SOLAR RADIATION, INCIDENT AND ABSORBED, W/m**2
SIG       = SIGMA--STEFAN-BOLTZMAN CONSTANT, 5.6697E-08
              W/(m**2*K**4)
T         = NUMBER OF HOURS STARTING AT MIDNIGHT ON FIRST
              SIMULATION DAY, H
TAMB      = AMBIENT DRY BULB TEMPERATURE, F, C OR K
TE(T)     = CALCULATED EQUIVALENT ROOF TEMPERATURE =(Tr), C
Tr(T)     = ROOF SURFACE TEMPERATURE AT HOUR T, C OR K
Tri       = CALCULATED INSIDE ROOF SURFACE TEMPERATURE, K
Try(T)    = TRIAL ROOF SURFACE TEMPERATURE, K
TSET      = AMBIENT ROOM/AIR PLENUM TEMPERATURE, C OR K
TW        = AMBIENT WET BULB TEMPERATURE, F, C OR K
W         = OMEGA--HUMIDITY RATIO, MASS OF WATER PER UNIT
              MASS OF DRY AIR
```

APPENDIX B
UNCERTAINTY ANALYSIS

To estimate the accuracy of the predicted results it is necessary to quantify the uncertainty of the individual variables and its effect on the uncertainty of the model results. In this thesis the result is the prediction of the heat gain through the roof, q_e. The variables include ambient temperature, humidity ratio, solar heat flux at the roof surface, inside and outside convective heat transfer coefficients, thermal resistance of the roof, and net radiative heat exchange with the sky.

The uncertainty analysis method chosen is the sequential perturbation of the data reduction program described in Appendix A. This method is described in detail by Moffat [19]. This method is based on determining the effect of each variable's uncertainty on the baseline predicted result. After the result of the baseline data set are calculated results are determined "once more for each variable, with the value of the variable increased by its uncertainty interval (and all other [variables] returned to their baseline values)". [19] The difference between the returned perturbed results and the baseline represents the contribution of each variable's uncertainty on the uncertainty of the result's

overall uncertainty. The uncertainty of the result is determined by squaring each contribution, summing, and taking the square root.

The expression used to calculate the uncertainty W of a function is

$$W=\left\{\sum_{i=1}^{n}(W_{x_i})^2\right\}^{\frac{1}{2}} \qquad \text{(B-1)}$$

where x_i is any of the variables which quantify the function.

The uncertainty interval for each variable has been estimated based on Somasundaram et al. [5] and Houghten et al.[1] . The results of the sequential perturbation for the roof-spray cooled concrete roof at Pittsburgh are provided in Table B.1.

Table B.1 Uncertainty Analysis by Sequential Perturbation for Concrete Roof at Pittsburgh

Case/ Perturbed Variable	Uncertainty Interval	Perturbed Result (W/m^2)	Difference From Baseline (W/m^2)
Baseline		-4.73	
T_a	0.5 K	-4.28	0.45
ω	0.001 $kg_{water}/kg_{dry\ air}$	-4.72	0.01
q_{solar} and α	10 W/m^2	-4.27	0.46
h_i	2 $W/(m^2\ K)$	-4.71	0.02
h_o	4 $W/(m^2\ K)$	-4.28	0.45
R_r	0.05 $m^2\ K/W$	-4.42	0.31
T_{set}	0.5 K	-5.42	0.69
δR	10 W/m^2	-5.13	0.39

The calculation of the total uncertainty, W, is shown by

$$W= \{(0.45)^2+(0.01)^2+(0.46)^2+(0.02)^2+(0.45)^2+(0.31)^2+(0.69)^2+(0.39)^2\}^{0.5}$$

which yields an uncertainty, W, of 1.2 W/m^2. Similar calculations for the other roofs yielded uncertainties of 0.2 W/m^2 for the predicted 0.40 W/m^2 predicted average roof heat gain for the spray cooled roof at Bryan, Texas, 1.2 W/m^2 for the predicted 2.4 W/m^2 predicted average for the dry roof at Bryan, and 1.4 W/m^2 for the predicted -4.2 W/m^2 average for the spray cooled pine plank roof at Pittsburgh.

REFERENCES

1. Houghten, F.C., Gutberlet, C., and Olson, H.T., "Summer Cooling Load as Affected by Heat Gain Through Dry, Sprinkled, and Water Covered Roofs," ASHVE Transactions, Vol. 46, 1940, pp. 231-246.

2. Yellott, J.I., "Roof Cooling with Intermittent Sprays," ASHRAE 73rd Annual Meeting in Toronto, Ontario, Canada, June 27-29, 1966.

3. Tiwari, G.N., Kumar, A., and Sodha, M.S., "A Review of Cooling by Water Evaporation Over Roof," Energy Conversion and Management, Vol. 22, 1982, pp. 143-153.

4. Carrasco, A., Pittard, R., Kondepudi, S.N., and Somasundaram, S., "Evaluation of a Direct Evaporative Roof Spray Cooling System," Proceedings of the Fourth Annual Symposium on Improving Building Energy Efficiency in Hot and Humid Climates, Houston, Texas, 1987, pp. 94-101.

5. Somasundaram, S. and Carrasco, A., "An Experimental and Numerical Modeling of a Roof-Spray Cooling System," ASHRAE Transactions, Vol. 94, Part 2, 1988, pp. 1091-1107.

6. Kondepudi, S.N., "A Simplified Analytical Method to Evaluate the Effects of Roof Spray Evaporative Cooling," Energy Conversion and Management, Vol. 34, 1993, pp. 7-16.

7. Spitler, J.D., and McQuiston, F.C., Cooling and Heating Load Calculation Manual, American Society of Heating, Refrigerating and Air-Conditioning Engineers, Atlanta, Georgia, 1992.

8. Mathur, G.D., "Predicting Water Vapor Saturation Pressure," Heating/Piping/Air Conditioning, Vol. 61, April 1989, pp. 103-104.

9. ASHRAE Handbook, Fundamentals, Chapter 6, American Society of Heating, Refrigerating and Air-Conditioning Engineers, Atlanta, Georgia, 1989.